



Supplement of

Regional CO₂ inversions with LUMIA, the Lund University Modular Inversion Algorithm, v1.0

Guillaume Monteil and Marko Scholze

Correspondence to: Guillaume Monteil (guillaume.monteil@nateko.lu.se)

The copyright of individual parts of the supplement might differ from the article licence.

Supplementary figures

- Figure SI1: Monthly distribution of the prescribed prior uncertainties in simulations SRef, SE.3H, SE.3Hcst and SE.x2
- Figure SI2: Same as Figure 5a of the article, but with the individual sensitivity test results.
- Figure SI3: Same as Figure 8a of the article, but with the individual sensitivity test results.
- Figure SI4:
 - Figure SI4a: Monthly maps of the posteriors in the eight OSSEs
 - Figure SI4b: Monthly maps of the posterior errors (wrt the known truth) in the OSSEs
 - Figure SI4c: Monthly maps of the flux adjustments by the OSSEs
- Figure SI5:
 - Figure SI5a: Monthly maps of the posteriors in the eight inversions with real observations.
 - Figure SI5b: Monthly maps of the flux adjustments in the eight inversions with real inversions.
- Table SI1: List of sites used in the TM5 inversion (background).

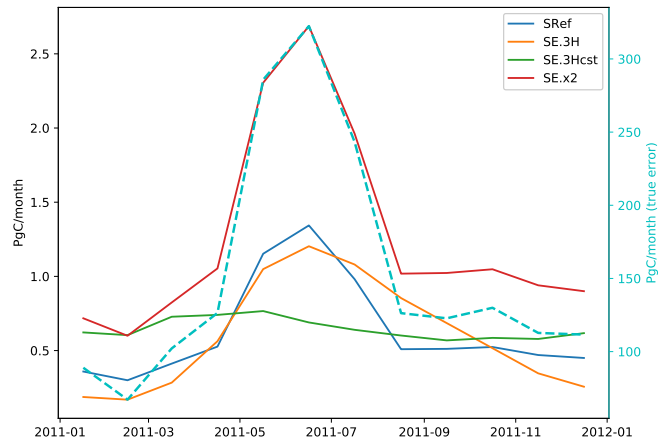


Figure SI1: Left axis: monthly uncertainty in four of the OSSEs, aggregated on the inversion domain (SO.A, SO.P, SC.100 and SC.500 have the same net uncertainty than SRef and are not displayed here). Right axis (cyan, dashed-line): “true” prior error (i.e. sum of the absolute differences between the prior and the truth).

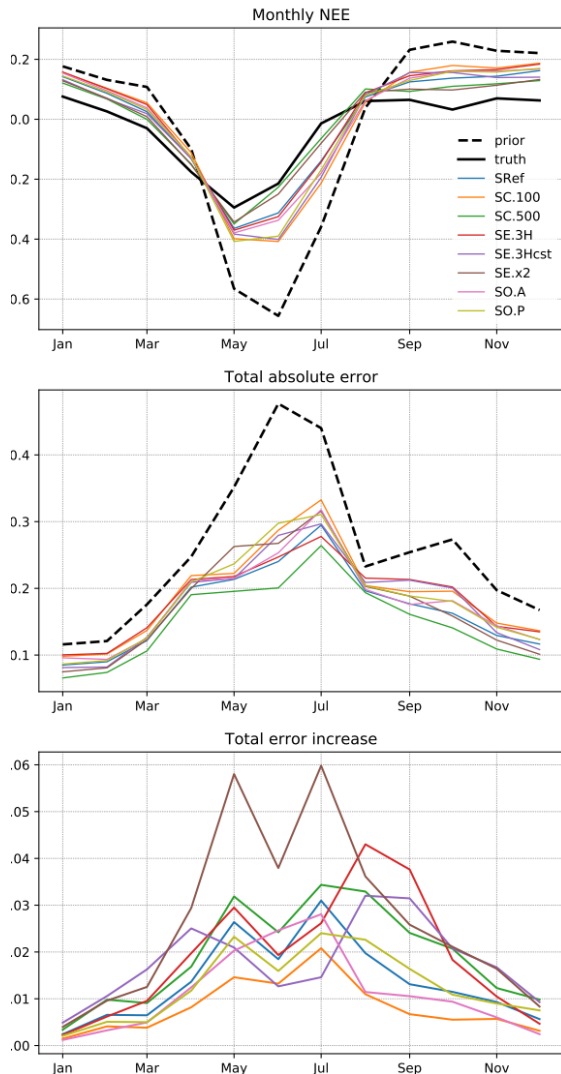


Figure SI2: Top: monthly NEE, in the prior, truth and posteriors for the OSSEs; Center: total absolute error (i.e. sum of the absolute deviations from the truth) for the prior and for each OSSE posterior; Bottom: total error increase (i.e. sum of the positive component of the error reduction), for each OSSE posterior

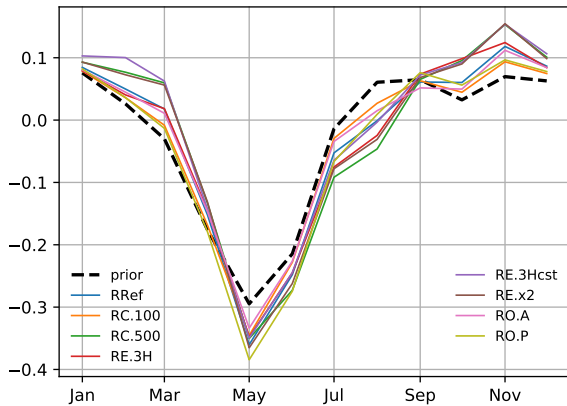


Figure SI3: monthly NEE for the inversions using real observations



Figure SI4a: Monthly posterior NEE in the eight OSSEs (the color range varies month to month, but is the same for all simulations)



Figure SI4b: Monthly posterior error (wrt truth) in the eight OSSEs (the color range varies month to month, but is the same for all simulations).



Figure SI4c: Monthly flux adjustment (posterior minus prior) in the eight OSSEs (the color range varies month to month, but is the same for all simulations).



Figure SI5a: Monthly posterior NEE in the eight sensitivity inversions with real observations (the color range varies month to month, but is the same for all simulations)



Figure SI5b: Monthly flux adjustment (posterior minus prior) in the eight sensitivity inversions with real observations (the color range varies month to month, but is the same for all simulations).

Table SI1: List of sites used in the TM5 inversion for computing the background concentrations. The last column marks sites that are also used in the regional inversion (RI)

code	lat	lon	name	RI
ALT	82.45	-60.51	Alert, Nunavut	
ASC	-7.97	-14.4	Ascension Island	
ASK	23.26	5.63	Assekrem	
AZR	38.77	-27.37	Terceira Island, Azores	X
BAL	55.35	17.22	Baltic Sea	X
BHD	-41.41	174.87	Baring Head Station	
BKT	-0.2	100.32	Bukit Kototabang	
BMW	37.26	-64.88	Tudor Hill, Bermuda	
BRW	71.32	-156.61	Barrow Atmospheric Baseline Observatory	
BSC	44.18	28.66	Black Sea, Constanta	X
CBA	55.21	-162.72	Cold Bay, Alaska	
CES	51.97	4.93	Cesar, Cabauw	X
CGO	-40.68	144.69	Cape Grim, Tasmania	
CHR	1.7	-157.15	Christmas Island	
CIB	41.81	-4.93	Centro de Investigacion de la Baja Atmosfera (CIBA)	X
CMN	44.17	10.68	Monte Cimone	X
CRP	52.18	-6.37	Carnsore Point	X
CRZ	-46.43	51.85	Crozet Island	
DRP	N/A	N/A	Drake Passage	
DSI	20.7	116.73	Dongsha Island	
EIC	-27.16	-109.43	Easter Island	
ELL	42.57	0.95	Estany Llong	X
GMI	13.39	144.66	Mariana Islands	
HBA	-75.6	-26.21	Halley Station, Antarctica	
HEI	49.42	8.67	Heidelberg	X
HPB	47.8	11.02	Hohenpeissenberg	X
HSU	41.05	-124.75	Humboldt State University	
HUN	46.95	16.65	Hegyhatsal	X
IZO	28.31	-16.5	Izana, Tenerife, Canary Islands	
JFJ	46.55	7.99	Jungfraujoch	X
KAS	49.23	19.98	Kasprowy Wierch, High Tatra	X
KEY	25.67	-80.16	Key Biscayne, Florida	
KUM	19.74	-155.01	Cape Kumukahi, Hawaii	
LLB	54.95	-112.45	Lac La Biche, Alberta	
LLN	23.47	120.87	Lulin	
LMP	35.52	12.62	Lampedusa	X
LUT	53.4	6.35	Lutjewad	X
MEX	18.98	-97.31	High Altitude Global Climate Observation Center	
MHD	53.33	-9.9	Mace Head, County Galway	X
MID	28.21	-177.38	Sand Island, Midway	
MKN	-0.06	37.3	Mt. Kenya	
MLO	19.54	-155.58	Mauna Loa, Hawaii	
NAT	-5.8	-35.19	Farol De Mae Luiza Lighthouse	
NMB	-23.58	15.03	Gobabeb	
NWR	40.05	-105.59	Niwot Ridge, Colorado	
OPE	48.56	5.5	Observatoire perenne de l'environnement	X
OKX	50.03	11.81	Ochsenkopf	X
PAL	67.97	24.12	Pallas-Sammaltunturi, GAW Station	X

POC	N/A	N/A	Pacific Ocean	
PSA	-64.92	-64	Palmer Station, Antarctica	
PTA	38.95	-123.74	Point Arena, California	
PUI	62.91	27.65	Puijo	X
RPB	13.16	-59.43	Ragged Point	
SDZ	40.65	117.12	Shangdianzi	
SEY	-4.68	55.53	Mahe Island	
SGP	36.61	-97.49	Southern Great Plains, Oklahoma	
SHM	52.71	174.13	Shemya Island, Alaska	
SMO	-14.25	-170.56	Tutuila	
SPO	-89.98	-24.8	South Pole, Antarctica	
SSL	47.92	7.92	Schauinsland, Baden-Wuerttemberg	X
SUM	72.6	-38.42	Summit	
SYO	-69.01	39.59	Syowa Station, Antarctica	
TAP	36.74	126.13	Tae-ahn Peninsula	
THD	41.05	-124.15	Trinidad Head, California	
TIK	71.6	128.89	Hydrometeorological Observatory of Tiksi	
TRN	47.96	2.11	Trainou	X
TTA	56.56	-2.99	Tall Tower Angus	X
USH	-54.85	-68.31	Ushuaia	
UTA	39.9	-113.72	Wendover, Utah	
UUM	44.45	111.1	Ulaan Uul	
WAO	52.95	1.12	Weybourne, Norfolk	X
			Weizmann Institute of Science at the Arava Institute,	
WIS	29.96	35.06	Ketura	X
WLG	36.29	100.9	Mt. Waliguan	
WPC	N/A	N/A	Western Pacific Cruise	
ZEP	78.91	11.89	Ny-Alesund, Svalbard	X